

Molecular docking, synthesis, and biological evaluation of naphthoquinone as potential novel scaffold for H5N1 neuraminidase inhibition

Garima Sharma, S. Vasanth Kumar & Habibah A. Wahab

To cite this article: Garima Sharma, S. Vasanth Kumar & Habibah A. Wahab (2016): Molecular docking, synthesis, and biological evaluation of naphthoquinone as potential novel scaffold for H5N1 neuraminidase inhibition, Journal of Biomolecular Structure and Dynamics, DOI: [10.1080/07391102.2016.1274271](https://doi.org/10.1080/07391102.2016.1274271)

To link to this article: <http://dx.doi.org/10.1080/07391102.2016.1274271>



Accepted author version posted online: 25 Dec 2016.



Submit your article to this journal [↗](#)



View related articles [↗](#)



View Crossmark data [↗](#)

Publisher: Taylor & Francis

Journal: *Journal of Biomolecular Structure and Dynamics*

DOI: <http://dx.doi.org/10.1080/07391102.2016.1274271>

Molecular docking, synthesis, and biological evaluation of naphthoquinone as potential novel scaffold for H5N1 neuraminidase inhibition

Garima Sharma^{1,2}, S. Vasanth Kumar¹, Habibah A.Wahab^{2,*}

¹ Department of Chemistry, Karunya University, Coimbatore, India

² School of Pharmaceutical Sciences, Universiti Sains Malaysia, 11800 USM, Penang, Malaysia

* Corresponding author: E-mail: habibahw@usm.my, Tel.: +604-653-2206; +604 653-2238;
Fax: +604 657-0017.

Abstract

A series of dimeric naphthoquinones containing natural 2-hydroxy-1,4-naphthoquinone moiety was designed, synthesized and evaluated against neuraminidase of H5N1 virus. *p*-Hydroxy derivatives showed higher inhibition when compared to *p*-halogenated compounds. Molecular docking studies conducted with H5N1 neuraminidase clearly demonstrated different binding modes of the most active compound onto the open and closed conformations of loop 150. The results thus provide not only evidences of a novel scaffold evaluated as inhibitor, but also a rational explanation involving molecular modeling and the role of loop 150 in the binding.

Keywords: Neuraminidase; H5N1; Molecular docking; Naphthoquinone; Lawsone

1. Introduction

Influenza has infected millions of people globally. It is a major global health problem, and the related potential financial, societal and political impacts cannot be understated (Nicholson, 1996). Influenza is caused by the influenza virus, which has evolved and mutated over time, posing serious challenges in developing effective therapies (Yusuf et al., 2016). H5N1 and H1N1 are among the most dangerous influenza-A types, evidently spreading in epidemic and pandemic scales. H5N1, a type of virulent influenza spreading through birds that can be a pandemic threat to human (Horimoto & Kawaoka, 2001), has caused much concerns when 43 deaths associated with this infection in 2005 were reported in the South East Asian countries. These concerns were compounded by the confirmation from The World Health Organization (WHO) that the pandemic spread to over 220 countries with more than 39 million cases and 15,417 deaths worldwide as reviewed by (Fajardo-Dolci et al., 2010).

Influenza viruses can be classified into A, B and C based on their antigenic differences. Subtype A is the most therapeutically studied due to its pathogenic implications. The influenza viruses are negative-sense single stranded RNA viruses from the family *Orthomyxoviridae*. The genome of the virus contains eight different proteins, which are haemagglutinin (HA), neuraminidase (NA), matrix protein1 (M1), M2 proton channel, nucleoprotein (NP), non-structural protein1 (NS1), nuclear export protein (NEP) and RNA polymerases. Due to segmented nature of this genome, the surface glycoproteins HA and NA can occur in different combinations on different viruses and in different hosts e.g. sixteen HA subtypes [H1-H16] and nine NA [N1-N9] have been discovered till date. HA is the receptor-binding and membrane fusion glycoprotein of the influenza virus (Yusuf et al., 2013). HA is solely responsible for the viral entry into host cell and release of viral ribonucleo-protein complexes while NA cleaves terminal neuraminic acid (also called sialic acid) residues from glycan structures on the surface of the infected cell. This

promotes the release of progeny viruses and the spread of the virus from the host cell to uninfected surrounding cells (Skehel & Wiley, 2000).

Insights into the life cycle of the virus have revealed NA as a molecular target of therapeutic importance, which can be utilized for structure based drug design purposes due to its important role in replication of the virus (Gong, Xu, & Zhang, 2007; Gubareva, Kaiser, & Hayden, 2000; Laver & Garman, 2002). The four NA inhibitors currently in use in the treatment of influenza are zanamivir (Relenza™), oseltamivir (Tamiflu™) (Varghese, Mckimmbreschkin, Caldwell, Kortt, & Colman, 1992), peramivir (Sugaya, Kohno, Ishibashi, Wajima, & Takahashi, 2012) and most recently, laninamivir (Sugaya & Ohashi, 2010). However, due to the development of resistance (Stephenson et al., 2009) and side effects (Hurt, Holien, & Barr, 2009) associated with these drugs, significant efforts are being put to discover novel inhibitors against influenza.

Several series of NA inhibitors originating from a variety of scaffolds have been developed using structure based methods relying on crystallographic data including pyrrolidines (Wang et al., 2001), cyclopentanes (Babu et al., 2000), tetrahydrofurans (Wang et al., 2005) and benzenes (Singh et al., 1995). Other than synthetic moieties, recently, Grienke and co-workers (Grienke et al., 2012) compiled and reported a plethora of natural scaffolds. Other reports include coumarins and coumestanes (Ryu et al., 2010), diarylheptanoids (Grienke et al., 2010), auronos, biflavonoids and catechins (Li et al., 2007; Liu, Wang, Lee, Wang, & Du, 2008; Mercader & Pomilio, 2010), chalcones, flavanones and flavanonoles (Dao et al., 2010), oligostibenes (Grienke et al., 2010), isoprenoid (Grienke et al., 2010), phenyl propanoids (Zhang et al., 2010) and ferulic acid as well as vanillin derivatives (Hariono et al., 2016) as potential molecules which inhibit neuraminidase considerably.

Our aim is to explore and develop novel class of inhibitors derived from natural resources with the potential to inhibit H5N1 neuraminidase. Previously, our group has demonstrated successful docking application in identifying seven plants with potential neuraminidase activity (Ikram et al., 2015). The present work is inspired by some Cibacron Blue 3GA (CB3GA) based dyes and Shikonin (naturally occurring naphthoquinone) derivatives which are active against glycosyl hydrolase 33 (bacterial and simple eukaryotic sialidases) and 34 sialidases (viral sialidases) (Kim et al., 2012; Platis, Smith, Huyton, & Labrou, 2006). A predictive assumption was framed based

on these experimental evidences that the chemical moieties presented in the current study might also be therapeutically active against H5N1 influenza neuraminidase. Molecular docking studies provided evidence of strong binding interactions with the important amino acids in the active site and also demonstrated different binding modes of the most active compound (compound **2**) onto the open and closed conformations of loop-150. Derivatives of 2-hydroxy-1,4-naphthoquinone (popularly known as lawsone as well as hennotannic acid, a natural red orange dye compound found in the leaves of *Lawsonia inermis* used for hair and skin dyes since ancient time), were synthesized and found to be active in H5N1 neuraminidase inhibitory bioassay. It is therefore proposed that this type of compounds can pave the way towards further development of novel neuraminidase inhibitors. Previously, this class of compounds have been evaluated against HIV (Mazumder et al., 1996) and leishmaniasis therapeutic targets (Sharma, Chowdhury, Sinha, Majumder, & Kumar, 2014). To the best of authors' knowledge, naphthoquinone based H5N1 neuraminidase inhibitors have not been reported so far.

2. Experimental Section

2.1. Materials, methods and Instruments

All chemicals except H5N1 neuraminidase used in the current work were purchased from Sigma Aldrich Chemical Company and were used without purification. Lawsone and lawsone-dimer were obtained from Sigma Aldrich, Bangalore, India. H5N1 neuraminidase was obtained from SINBIO (China). MUNANA [2'-(4-methylumbelliferyl)- α -D-N-acetylneuraminic acid, sodium salt hydrate], MES [2-(N-morpholino)ethanesulphonic acid, and DANA [2,3-didehydro-2-deoxy-N-acetylneuraminic acid] were obtained from Sigma (Malaysia). Solvents were used as obtained from the supplier (Merck Chemical Company, Bangalore, India) or redistilled as necessary. Thin layer chromatography was performed on ready-made sheets procured from Merck Chemical Company (Bangalore, India). Melting points were measured on capillary melting point apparatus and were uncorrected. Mass spectra were recorded on a QSTAR Q-TOF AbSciex Corporation, Ontario, Canada. ^1H NMR spectra & ^{13}C NMR were recorded in DMSO with 400 MHz on a BRUKER Advance liquid state NMR, Bangalore, India. TMS (Trimethylsilane) was used as an internal standard and the chemical shifts (δ) were reported in ppm. IR spectra (KBr discs) were recorded on a SHIMADZU FT-IR 8400-S spectrophotometer, Mumbai, India. GOLD 5.1

Software, CCDC, UK (Jones, Willett, & Glen, 1995) was used for docking studies. PyMOL [www.pymol.org] and Discovery Studio visualizer was utilized for the purpose of visualization.

2.2. Molecular docking studies

Docking studies were performed using GOLD 5.1 program. Crystal structures of H5N1 neuraminidase (PDB ID: 2HU4 and 2HTY) were used for docking studies. The co-crystallized ligand (G39) in PDB ID (2HU4) (Russell et al., 2006) was redocked into the active site to validate the docking protocol. The RMSD between the original and the redocked ligand was found to be 0.454 Å (**Figure 1**).

Prior to synthesis, the compounds were designed and virtually screened by docking into the active site of PDB ID (2HU4) which has a loop-150 closed conformation. However, crystal structure of open loop-150 H5N1 neuraminidase PDB ID (2HTY) (Russell et al., 2006) was also used to study the interaction with only the best compound (compound **2**) for the sake of comparison of binding poses and interactions. All the water molecules and co-crystallized ligands (as and where present) were removed from the PDB protein structures and were loaded in the Hermes module of GOLD. Subsequently hydrogen atoms were also added. Preparation of protein and ligands (removal of water molecule, extraction of original ligands from the protein active site, addition of hydrogen and protonation state of the charge group) were done with GOLD as per default settings. The histidine protonation states were also determined and fixed in the protein structure. The binding site was determined using the previous knowledge of the original ligand interaction site (Russell et al., 2006). In docking simulations each ligand was kept flexible but the amino acid residues of the proteins were held rigid. For the simulation runs, default parameter values were taken. The selection of atoms in the active site within 6 Å of the original ligand was chosen as default. The minimum genetic algorithm run of 10,000 was selected. The number of generated poses was set to 10 and top ranked solutions were kept, with

the early termination option turned on. The Chemscore was selected for scoring function. The ChemScore fitness function incorporates the total free energy change that occurs on ligand binding that was trained by regression against binding affinity data for 82 complexes. The fitness function also takes into account a protein-ligand atom clash term, an internal energy term, hydrophobic-hydrophobic contact area, hydrogen bonding, ligand flexibility and metal interaction (Eldridge, Murray, Auton, Paolini, & Mee, 1997; Murray, Auton, & Eldridge, 1998). The results were saved in mol2 file for graphical analysis.

[Figure 1 here]

2.3. General Procedure for the Preparation of 3,3'-(arylmethylene)bis(2-hydroxynaphthalene-1, 4-dione) analogues (1-13)

The compounds were synthesized in aqueous medium according to the procedure described by Tisseh & Bazgir (Tisseh & Bazgir, 2009) and were appropriately characterized. Briefly, a mixture of 2-hydroxynaphthalene-1,4-dione (2 mmol), substituted aromatic aldehyde (1 mmol) and LiCl (1 mmol) in refluxing water (5 ml) was stirred for 12 hours and the reaction was monitored by TLC. After completion of the reaction, the reaction mixture was filtered and the precipitate washed with water and then with ethanol to afford the pure products **1-13** (Scheme 1).

[Scheme 1 here]

2.4. Biological Studies

2.4.1. Preparation of Stock solutions

325 mM MES buffer: 31.72 g MES + 500 mL deionized water (ddH₂O), 100 mM CaCl₂: 1.11 g CaCl₂ + 100 mL deionized water (ddH₂O), 1M Glycine: 37.5 g Glycine + 500 mL deionized water (ddH₂O) pH 10.7

2.4.2. Drug solutions

Soluble drugs: 1 mg compounds diluted in 1ml MES Buffer [1000 $\mu\text{L}/\text{mL}$].

Partially soluble drugs: 1mg compounds diluted in 25 μL 100% DMSO + 975 μL MES Buffer = [1000 $\mu\text{L}/\text{mL}$]. Thus concentration of compounds stock prepared: [1000 $\mu\text{L}/\text{mL}$].

2.4.3. Neuraminidase assay

Neuraminidase assays were performed by modifying the method of Potier et al (Potier, Mameli, Belisle, Dallaire, & Melancon, 1979). Neuraminidases from bacterial and viral H5N1 in MES buffer were used as the enzyme in the study. MUNANA (Sigma, M8639) was prepared by 32.5mM MES buffer (pH6.5) and used as the substrate. The compounds were dissolved in 2.5% DMSO and diluted with MES buffer to make up the corresponding concentrations (250 $\mu\text{L}/\text{mL}$, 0.12 $\mu\text{L}/\text{mL}$, and 12 concentrations). Twenty-five microliters of neuraminidase was added in 25 μL of sample solution mixed with buffer in 96-well micro plates. Fifty microlitres of MUNANA was subsequently added and incubated at 37°C. After one hour, 4-methylumbelliferone was quantified fluorometrically on a Modulus Microplate Reader (Turner Biosystem, USA). The excitation and emission wavelengths were set at 365 nm and 450 nm, respectively. The percentages of neuraminidase inhibition of the compounds were determined as $100 - [\text{percentage activity} / \text{positive control} \times 100]$. DANA was used as the standard inhibitor for positive control in the bioassay.

3. Results and Discussion

3.1. Docking Studies

The docking studies for all ligands were performed with PDB (2HU4) as target structure to investigate the key interactions responsible for the potency of this class of inhibitors. Chemscore of all the selected ligands were showed (Table 1) and (Figure 2) shows the all the ligands superimposed in the binding site of PDB (2HU4).

[Table. 1 here]

[Figure 2 here]

The binding pocket of the H5N1 avian influenza NA in both the open (PDB ID (2HTY)) and close (2HU4) conformations was defined to include Arg 371, Tyr 347, Arg 292, Asn 224, Glu 276, Ser 246, Glu 277, Arg 224, Ile 222, Arg 152, Ser 179, Trp 178, Asp 151, Glu 119, Arg 118, Arg 156 and Tyr 406 (Russell et al., 2006). As compound **2** proved to be experimentally the most active, this compound was chosen for further analysis.

Molecular docking studies demonstrated a plausible mechanism for the interaction of compound **2** in open and closed conformations. Compound **2** makes hydrogen bonds with Arg 118, Arg 371, Tyr 406, Glu 277, Asp 151 and Arg 152 (Figure 3(A)). There are also possible hydrophobic contacts between this compound and Tyr 347 with open conformation (Figure 5(C)). On the other hand in the closed conformation, the binding pocket of the H5N1 avian influenza NA was also defined to include the same set of amino acids as described above (Figure 3(B)).

A marked change was observed in the binding mode of compound **2** upon docking in the closed conformation of loop 150. The ligand is shown to be protruding with the aryl group moving far from Tyr 347, thus losing the hydrophobic contact with this residue. The heavy atom RMSD of the docked poses of this particular ligand between loop 150 open and closed conformations were observed to be 1.78Å. Although the hydrogen bond interactions observed in open conformation binding mode are retained but the ligand moved closer to residues Asp 151 and Arg 152. Distance of Asp 151 and Arg 152 in closed conformation were 2.086 Å and 2.077 Å (Figure 4 (A)), respectively, whereas in the open conformation, were 1.562 Å and 1.564 Å (Figure 4 (B)). This might be due to the hinge effect with the closure of loop 150, as observed from one of the aryl moieties that form hydrophobic interaction with the side chain of Arg 224. This is a fact which is commonly observed in oseltamivir carboxylate's binding (PDB: 2HU4, Figure 5), as well as in the binding of DANA (PDB: 1NNB) (Stoll et al., 2003). However, the hydrophobic interaction observed is not as elaborate as to cover the sub-pocket consisting of Trp 178, Ile 222 and Arg 224 as described previously (Stoll et al., 2003) but it is restricted only to Arg 224. It is also highly possible that there are chances for the *p*-Hydroxyl group of the aryl moiety of this

compound to form a hydrogen bond interaction with Ser 246 during the actual molecular movement (Figure 3(B)). In contrast, lawsone does not bind with any of the residues in the arginine triad (Arg 118, Arg 371 and Arg 292) but showed hydrogen bond interaction with Glu 277 and most probably making π -cation interaction with Arg 224. Thus, it was not surprising that this compound showed low neuraminidase inhibitory property.

[Figure 3 here]

[Figure 4 here]

3.2. Synthesis

All the thirteen compounds (Scheme 1) have been synthesized according to method described by (Tisseh & Bazgir, 2009) in pure form whereas compound no. **1**, **3**, **4**, **6**, **9** and **12** were not reported previously in literature. Characterization of the compounds was done through physical and spectroscopy techniques such as melting point, thin layer chromatography, infra-red, ^1H NMR, ^{13}C NMR spectroscopies and mass spectrometry.

3,3'((4-Hydroxy-3-methoxyphenyl)methylene)bis(2-hydroxynaphthelene-1,4-dione)(1). reddish brown powder, mp 180-182°C; IR (KBr) (ν_{max}): 3326, 2920, 2842, 1673, 1585, 1033 cm^{-1} ; ^1H NMR (DMSO- d_6): δ_{H} 5.94 (s, 1H) 6.60 (d, $J=2$ Hz, 2H) 6.81 (s, 1H) 7.22 (m, 1H) 7.76-7.85 (m, 4H) 7.92-7.95 (dd, $J=7.6, 1.2$ Hz, 2H), 7.97-8.00 (dd, $J=7.2, 1.2$ Hz, 2H) ppm; ^{13}C NMR (DMSO): 30.70, 52.40, 55.01, 56.17, 107.73, 109.49, 117.72, 122.10, 127.23, 128.82, 131.49, 132.18, 133.80, 134.5, 144.6, 146.9, 156.1, 181.2, 183.6 ppm; MS (Mass) m/z : 483 $[\text{M}+\text{H}]^+$.

3,3'((4-Hydroxy-phenyl)methylene)bis(2-hydroxynaphthelene-1,4-dione) (2). red orange powder, mp 175-177 °C; IR (KBr) (ν_{max}) : 3349, 3336, 1673, 1585 cm^{-1} ; ^1H NMR (DMSO- d_6) : δ_{H} 5.95 (s, 1H) 6.57-6.59 (d, $J=6.8$ Hz, 2H), 7.00-7.02 (d, $J=8.4$ Hz, 2H) 7.75-7.84 (m, 5H) 7.92-7.99 (dd, $J=1.6, 1.2$ Hz) 9.02 (bs, 1H) ppm; ^{13}C NMR (DMSO): 36.85, 114.44, 123.69, 125.46, 125.95, 129.05, 129.82, 130.65, 132.20, 132.98, 134.55, 155.17, 156.21, 181.31, 183.56 ppm; MS (Mass) m/z : 453 $[\text{M}+\text{H}]^+$.

3,3'-((4-Hydroxy-3-ethoxyphenyl)methylene)bis(2-hydroxynaphthalene-1,4-dione) (**3**). brown powder, mp 190-192 °C; IR (KBr) (ν_{\max}): 3338, 2978, 2929, 1651, 1593, 1512, 1041 cm^{-1} ; ^1H NMR (DMSO- d_6): δ_{H} 1.22-1.25 (t, $J=11.2$ Hz) 3.87-3.91 (q, $J=5.6$ Hz, 2H) 5.9 (s, 1H) 6.59 (d, $J=0.8$ Hz, 2H) 6.79 (s, 1H) 7.75-7.85 (m, 4H) 7.92-7.93 (d, $J=7.2$ Hz, 2H) 7.97-7.99 (d, $J=6$ Hz, 2H) 9.8 (s, 1H); ^{13}C NMR (DMSO- d_6): 14.69, 32.43, 63.94, 113.29, 114.93, 119.42, 122.85, 125.01, 125.67, 130.90, 131.97, 133.31, 133.69, 144.35, 146.03, 183.70 ppm; MS (Mass) m/z : 495 $[\text{M-H}]^+$.

3,3'-((3,4-Di-hydroxy-phenyl)methylene)bis(2-hydroxynaphthalene-1,4-dione) (**4**). red-brown powder, mp 178-180 °C; IR (KBr) (ν_{\max}): 3377, 2916, 2848, 1670, 1647, 1591 cm^{-1} ; ^1H NMR (DMSO- d_6): δ_{H} 6.35 (m, 1H) 6.53 (m, 3H) 7.67 (td, 2H) 7.76 (td, 2H) 7.89 (m, 2H) 7.97 (dd, $J=4$ Hz 2H) 8.34 (s, 1H) 8.49 (s, 1H) ppm; ^{13}C NMR (DMSO- d_6): 32.12, 114.39, 114.95, 124.97, 125.66, 130.88, 131.76, 132.05, 133.70, 142.40, 144.46, 183.74 ppm; MS (Mass) m/z : 468 $[\text{M}^+]$.

3,3'-((3-Bromophenyl)methylene)bis(2-hydroxynaphthalene-1,4-dione) (**5**). yellow powder, mp 221-223°C; IR (KBr) (ν_{\max}): 3346, 1654, 1591 cm^{-1} ; ^1H NMR (DMSO- d_6): δ_{H} 6.00 (s, 1H) 7.12-7.18 (t, $J=8$ Hz, 1H) 7.28 (d, $J=8$ Hz, 1H) 7.35 (d, $J=8$ Hz, 1H) 7.44 (s, 1H) 7.90-8.10 (m, 8H) ppm; ^{13}C NMR (DMSO- d_6): 37.80, 121.82, 122.70, 126.01, 126.42, 127.81, 128.83, 130.10, 130.31, 131.12, 132.60, 133.50, 135.12, 144.42, 156.90, 181.60, 183.83 ppm; MS (Mass) m/z : 515.01 $[\text{M+H}]^+$.

3,3'-((4-Cyanophenyl)methylene)bis(2-hydroxynaphthalene-1,4-dione) (**6**). orange yellow powder, mp 195-197°C; IR (KBr) (ν_{\max}): 3510, 2901, 2229, 1674, 1597 cm^{-1} ; ^1H NMR (DMSO- d_6): δ_{H} 6.64 (s, 1H) 7.11-7.20 (dd, $J=8, 4$ Hz, 4H) 7.64-7.77 (m, 4H) 7.86-7.96 (dd, $J=8, 3.2$ Hz, 4H) ppm; ^{13}C NMR (DMSO- d_6): 32.64, 122.01, 125.09, 125.75, 127.54, 128.72, 129.25, 130.91, 131.85, 131.19, 133.72, 140.56, 174.44, 182.24, 183.41 ppm; MS (Mass) m/z : 462 $[\text{M+H}]^+$.

3,3'-((4-Chlorophenyl)methylene)bis(2-hydroxynaphthalene-1,4-dione) (**7**). orange powder, mp 180-182°C; IR (KBr) (ν_{\max}): 3337, 1674, 1597 cm^{-1} ; ^1H NMR (DMSO- d_6): δ_{H} 6.72 (s, 1H) 7.31-7.33 (d, $J=8$ Hz, 2H) 7.59-7.61 (d, $J=8$ Hz, 2H) 7.65-7.69 (m, 4H) 7.87-7.89 (d, $J=8$ Hz, 2H) 7.95-7.97 (d, $J=8$ Hz, 2H) ppm; ^{13}C NMR (DMSO- d_6): 33.60, 107.55, 19.22, 121.47, 125.14, 125.70,

127.93, 130.94, 131.66, 131.93, 133.13, 133.76, 148.16, 182.23, 183.28 ppm; MS (Mass) m/z : 471 [M+H]⁺.

3,3'-((4-Fluorophenyl)methylene)bis(2-hydroxynaphthalene-1,4-dione) (8). red powder, mp 200-205 °C; IR (KBr) (ν_{\max}): 3471, 1666, 1597, cm^{-1} ; ¹H NMR (DMSO-d₆): δ_{H} 6.60 (s, 1H) 6.93-6.96 (t, $J=7.2$ Hz, 2H) 7.09-7.12 (t, $J=6.4$ Hz, 2H) 7.64-7.96 (m, 8H) ppm; ¹³C NMR (DMSO-d₆): 32.36, 111.92, 114.17, 114.33, 122.31, 125.09, 128.47, 128.53, 130.95, 131.86, 133.25, 133.74, 137.34, 159.12, 161.03, 183.0 ppm; MS (Mass) m/z : 453 [M-H]⁺.

3,3'-((Thiophen-2-yl)methylene)bis(2-hydroxy-2,3-dihydronaphthalene-1,4-dione) (9). mustard yellow powder, mp 226-228 °C; IR (KBr) (ν_{\max}): 3400, 1674, 1590 cm^{-1} ; ¹H NMR (DMSO-d₆): δ_{H} 6.66-6.71 (m, 1H), 6.81 (dd, $J=4$, 2.8 Hz, 1H) 6.87 (s, 1H) 7.17 (d, $J=4$ Hz, 1H) 7.65-7.72 (m, 2H) 7.78 (td, 2H) 7.90 (d, $J=5.9$ Hz, 2H) 8.00 (d, $J=5.25$ Hz, 2H) ppm; ¹³C NMR (DMSO-d₆): 30.05, 122.92, 123.19, 123.97, 125.55, 125.58, 126.30, 131.32, 132.45, 133.62, 134.37, 147.12, 164.95, 182.36, 184.07 ppm; MS (Mass) m/z : 443[M+H]⁺.

3,3'-((3,4,5-Tri-methoxyphenyl)methylene)bis(2-hydroxynaphthalene-1,4-dione) (10). yellow powder, mp 178-180 °C; IR (KBr) (ν_{\max}): 3335, 2944, 2846, 1670, 1590, 1038 cm^{-1} ; ¹H NMR (DMSO-d₆): δ_{H} 3.60-3.68 (s, 9H) 5.96 (s, 1H) 6.55 (s, 2H) 7.76-7.86 (m, 4H) 7.93-8.02 (m, 4H) ppm; ¹³C NMR (DMSO): 37.84, 55.84, 59.87, 106.01, 123.06, 125.52, 126.01, 129.88, 132.20, 133.01, 134.57, 135.71, 136.42, 152.22, 156.24, 181.20, 183.54 ppm; MS (Mass) m/z : 527 [M+H]⁺.

3,3'-((4-Dimethylaminophenyl)methylene)bis(2-hydroxynaphthalene-1,4-dione) (11). brown red powder, mp 198-200 °C; IR (KBr) (ν_{\max}): 3498, 3333, 2919 2850, 1670, 1599, 1346 cm^{-1} ; ¹H NMR (DMSO-d₆) : δ_{H} 3.30 (s, 1H), 6.54-6.56 (t, $J=4$ Hz, 3H) 6.90-6.92 (d, $J=8$ Hz, 2H) 7.63-7.67 (m, 4H) 7.85-7.96 (m, 4H) ppm; ¹³C NMR (DMSO): 31.98, 40.49, 112.47, 122.90, 124.95, 125.63, 127.31, 129.20, 130.90, 131.70, 133.35, 133.64, 148.17, 164.53, 182.36, 183.71 ppm; MS (Mass) m/z: 480 [M+H]⁺.

3,3'-((4-Allyloxy)phenyl)methylene)bis(2-hydroxynaphthelene-1,4-dione) (**12**). yellow powder, mp 220-222 °C; IR (KBr) (ν_{\max}): 3433, 2939, 1658, 1604, 1435, 1334 cm^{-1} ; ^1H NMR (DMSO- d_6): δ 4.51 (s, 4H) 5.25-5.32 (m, 5H) 5.39-5.43 (d, $J=7.2$ Hz, 2H) 6.80 (d, $J=8.4$ Hz, 3H) 7.90-8.50 (m, 8H); ^{13}C NMR (DMSO): 22.02, 68.63, 69.00, 114.69, 118.09, 124.31, 126.37, 126.86, 127.46, 127.88, 129.65, 129.95, 130.84, 131.03, 133.83, 134.31, 134.90, 135.42, 135.70, 146.45 ppm; MS (Mass) m/z : 493 $[\text{M}+\text{H}]^+$.

3,3'-((3,4-Di-methoxyphenyl)methylene)bis(2-hydroxynaphthelene-1,4-dione) (**13**). red powder, mp 185-187 °C; IR (KBr) (ν_{\max}): 3335, 2944, 2846, 1674, 1550, 1338, 1038 cm^{-1} ; ^1H NMR (DMSO- d_6): δ_{H} 3.56-3.76 (m, 6H) 5.95 (br, s, 1H) 6.68-6.93 (m, 3H) 7.62-8.08 (m, 8H) ppm; ^{13}C NMR (DMSO): 37.88, 55.91, 56.00, 111.64, 113.31, 120.61, 123.93, 126.01, 126.49, 130.33, 132.68, 133.53, 133.57, 135.10, 147.49, 148.67, 156.53, 181.73, 184.09 ppm. MS (Mass) m/z : 497.12 $[\text{M}+\text{H}]^+$.

3.3. Biological studies

The synthesized compounds as well as lawsone and lawsone-dimer were tested for their inhibitory activity against bacterial neuraminidase of *Clostridium perfringens* at the concentration of 250 $\mu\text{g}/\text{mL}$. It was observed that most of the compounds showed $\geq 80\%$ inhibition on the bacterial NA (Table 2). Compounds **1**, **2**, **3**, **4**, carrying hydroxyl moiety ((R) phenyl = 4-hydroxy-3-methoxy, 4-hydroxy, 4-hydroxy-3-ethoxy and 3,4-di-hydroxy, respectively) showed inhibitions between 87-96.6% whereas 3,4-di-hydroxy moiety showed the highest percentage inhibition amongst all of the tested compounds. Compounds **5**, **6**, **7**, **8** ((R) phenyl = 3-bromo, 4-cyano, 4-chloro and 4-flouro, respectively) which have halogen groups demonstrated 89.0-91.2% inhibition against the bacterial NA while compound **9** with the thiophene group showed 81% inhibition. Compounds **10**, **11**, **12**, **13** ((R) phenyl = tri-methoxy, N-N-di-methyl amino, 4-allyloxy, di-methoxy respectively) showed 70.9-78.9% inhibition with compound **11** showing the lowest percentage of inhibition (70.9 %) amongst all. Lawsone and its dimer, respectively, showed 80.1% and 85.2 % inhibition. DANA which was used as a standard and positive control in this study, showed 93.0% inhibition against bacterial NA. In the bacterial NA assay, we noticed that hydroxyl and halogen moieties carrying compounds showed potent to good inhibition whereas methoxy group related compounds were showing average inhibition.

[Table 2 here]

Based on the initial screening results on the bacterial neuraminidase, ten best compounds with $\geq 80\%$ inhibition were selected, including lawsone and lawsone-dimer for viral H5N1 NA assay (Figure 6). All the ten compounds were active against H5N1 neuraminidase with four compounds, (compounds **1**, **2**, **4**) and lawsone, showed $> 80\%$ inhibition at 250 $\mu\text{g/mL}$.

[Figure 5 here]

Compounds **1** (percentage inhibition at 250 $\mu\text{g/mL}$ = 86%; IC_{50} : $29 \pm 0.9 \mu\text{M}$) and **2** (93.5%; $26.5 \pm 0.7 \mu\text{M}$) showed better inhibitory profile than DANA (94.8%; $34.82 \pm 1.32 \mu\text{M}$), see activity curves for compound 1 and 2 compared to DANA in Figure 6. Other compounds such as compounds **3**, **4**, **5**, **6** and **7**, lawsone and lawsone-dimer showed IC_{50} between 111-425 μM (Table 3). Although these compounds have similarity in structures with subtle differences in their phenyl group, compounds **3** and **4** exhibited greater IC_{50} (Compound **3**: $252 \pm 0.1 \mu\text{M}$; **4**: $111 \pm 0.20 \mu\text{M}$) compared to compounds **1** to **4** (Table 3).

[Figure 6 here]

[Table 3 here]

4. Conclusion

This work describes the molecular modeling, synthesis and evaluation of dimeric-naphthoquinones for the first time against influenza neuraminidase. The *p*-Hydroxyl derivative has been found to be the most active compound among all those screened. The molecular modeling studies suggest that the binding phenomenon of this class of compounds is in agreement with the experimentally proven key residues. Apart from this, as it appears to the authors, the loop 150 plays a major role in the formation of key interactions of the compounds in context. Docking studies with both open and closed conformation suggest better interactions upon loop150 closure. The present investigation demonstrates that the active molecules from this

study can be further developed as lead molecules with better inhibition characteristics towards H5N1 virus neuraminidase.

Acknowledgments

This work was partly supported by Universiti Sains Malaysia Research University grant (grant no-1: 304/PFARMASI/633069) and Malaysian Ministry of Science, Technology and Innovation, through Nutraceuticals R&D Initiative Grant (grant no-2: 09-05-IFN-MEB 004). GS and SVK thank the management and administration of Karunya University for their encouragement and support.

Conflicts of Interest

The authors declare no conflict of interest.

References

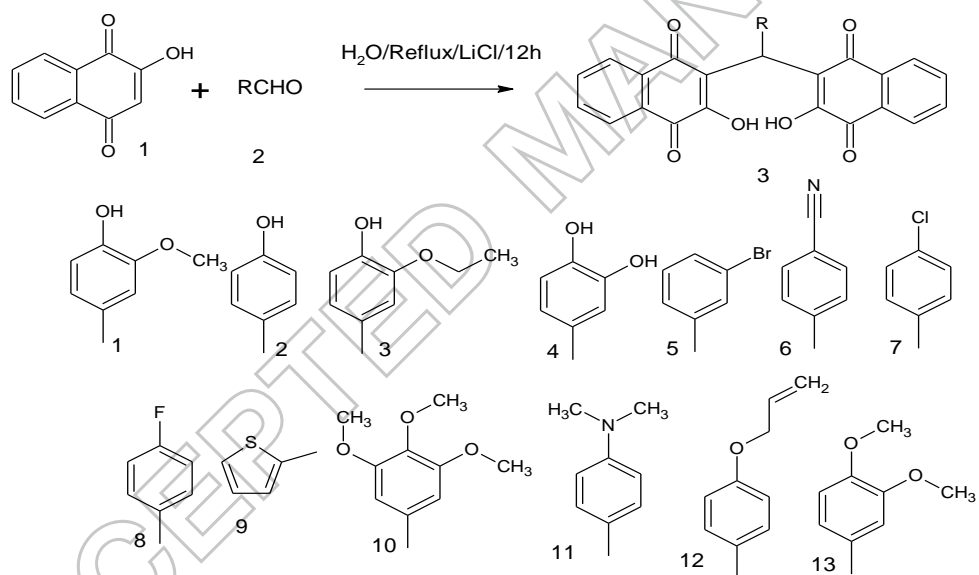
- Babu, Y. S., Chand, P., Bantia, S., Kotian, P., Dehghani, A., El-Kattan, Y. (2000). BCX-1812 (RWJ-270201): Discovery of a novel, highly potent, orally active, and selective influenza neuraminidase inhibitor through structure-based drug design. *Journal of Medicinal Chemistry*, 43(19), 3482-3486
- Dao, T. T., Tung, B. T., Nguyen, P. H., Thuong, P. T., Yoo, S. S., Kim, E. H. (2010). C-Methylated Flavonoids from *Cleistocalyx operculatus* and Their Inhibitory Effects on Novel Influenza A (H1N1) Neuraminidase. *Journal of Natural Products*, 73(10), 1636-1642
- Eldridge, M. D., Murray, C. W., Auton, T. R., Paolini, G. V., & Mee, R. P. (1997). Empirical scoring functions .1. The development of a fast empirical scoring function to estimate the binding affinity of ligands in receptor complexes. *Journal of Computer-Aided Molecular Design*, 11(5), 425-445. doi: Doi 10.1023/A:1007996124545
- Fajardo-Dolci, G., Gutierrez-Vega, R., Arboleya-Casanova, H., Villalobos, A., Wilson, K. S., Garcia, S. G. (2010). Clinical characteristics of fatalities due to influenza A (H1N1) virus in Mexico. *Thorax*, 65(6), 505-509
- Gong, J. Z., Xu, W. F., & Zhang, J. (2007). Structure and functions of influenza virus neuraminidase. *Current Medicinal Chemistry*, 14(1), 113-122

- Grienke, U., Schmidtke, M., Kirchmair, J., Pfarr, K., Wutzler, P., Durrwald, R. (2010). Antiviral Potential and Molecular Insight into Neuraminidase Inhibiting Diarylheptanoids from *Alpinia katsumadai*. *Journal of Medicinal Chemistry*, 53(2), 778-786
- Grienke, U., Schmidtke, M., von Grafenstein, S., Kirchmair, J., Liedl, K. R., & Rollinger, J. M. (2012). Influenza neuraminidase: A druggable target for natural products. *Natural Product Reports*, 29(1), 11-36
- Gubareva, L. V., Kaiser, L., & Hayden, F. G. (2000). Influenza virus neuraminidase inhibitors. *Lancet*, 355(9206), 827-835
- Hariono, M., Abdullah, N., Damodaran, K. V., Kamarulzaman, E. E., Mohamed, N., Syed Hassan, S. (2016). Potential New H1N1 Neuraminidase Inhibitors from Ferulic Acid and Vanillin: Molecular Modeling, Synthesis and in Vitro Assay *European Journal of Medicinal Chemistry*
- Horimoto, T., & Kawaoka, Y. (2001). Pandemic threat posed by avian influenza A viruses. *Clinical Microbiology Reviews*, 14(1), 129-+
- Hurt, A. C., Holien, J. K., & Barr, I. G. (2009). In Vitro Generation of Neuraminidase Inhibitor Resistance in A(H5N1) Influenza Viruses. *Antimicrobial Agents and Chemotherapy*, 53(10), 4433-4440
- Ikram, N. K. K., Durrant, J. D., Muchtaridi, M., Zalaludin, A. S., Purwitasari, N., Mohamed, N. (2015). A Virtual Screening Approach For Identifying Plants with Anti H5N1 Neuraminidase Activity. *Journal of Chemical Information and Modeling*, 55(2), 308-316
- Jones, G., Willett, P., & Glen, R. C. (1995). Molecular Recognition of Receptor-Sites Using a Genetic Algorithm with a Description of Desolvation. *Journal of Molecular Biology*, 245(1), 43-53
- Kim, J. Y., Jeong, H. J., Park, J. Y., Kim, Y. M., Park, S. J., Cho, J. K. (2012). Selective and slow-binding inhibition of shikonin derivatives isolated from *Lithospermum erythrorhizon* on glycosyl hydrolase 33 and 34 sialidases. *Bioorganic & Medicinal Chemistry*, 20(5), 1740-1748
- Laver, G., & Garman, E. (2002). Pandemic influenza: its origin and control. *Microbes and Infection*, 4(13), 1309-1316
- Li, X. F., Ohtsuki, T., Shindo, S., Sato, M., Koyano, T., Preeprame, S. (2007). Mangiferin identified in a screening study guided by neuraminidase inhibitory activity. *Planta Medica*, 73(11), 1195-1196
- Liu, A. L., Wang, H. D., Lee, S. M. Y., Wang, Y. T., & Du, G. H. (2008). Structure-activity relationship of flavonoids as influenza virus neuraminidase inhibitors and their in vitro anti-viral activities. *Bioorganic & Medicinal Chemistry*, 16(15), 7141-7147

- Mazumder, A., Wang, S. M., Neamati, N., Nicklaus, M., Sunder, S., Chen, J. (1996). Antiretroviral agents as inhibitors of both human immunodeficiency virus type 1 integrase and protease. *Journal of Medicinal Chemistry*, 39(13), 2472-2481
- Mercader, A. G., & Pomilio, A. B. (2010). QSAR study of flavonoids and biflavonoids as influenza H1N1 virus neuraminidase inhibitors. *European Journal of Medicinal Chemistry*, 45(5), 1724-1730
- Murray, C. W., Auton, T. R., & Eldridge, M. D. (1998). Empirical scoring functions. II. The testing of an empirical scoring function for the prediction of ligand-receptor binding affinities and the use of Bayesian regression to improve the quality of the model. *Journal of Computer-Aided Molecular Design*, 12(5), 503-519. doi: Doi 10.1023/A:1008040323669
- Nicholson, K. G. (1996). Impact of influenza and respiratory syncytial virus on mortality in England and Wales from January 1975 to December 1990. *Epidemiol Infect*, 116(1), 51-63
- Platis, D., Smith, B. J., Huyton, T., & Labrou, N. E. (2006). Structure-guided design of a novel class of benzyl-sulfonate inhibitors for influenza virus neuraminidase. *Biochemical Journal*, 399, 215-223
- Potier, M., Mamei, L., Belisle, M., Dallaire, L., & Melancon, S. B. (1979). Fluorometric Assay of Neuraminidase with a Sodium (4-Methylumbelliferyl-Alpha-D-N-Acetylneuraminat) Substrate. *Analytical Biochemistry*, 94(2), 287-296
- Russell, R. J., Haire, L. F., Stevens, D. J., Collins, P. J., Lin, Y. P., Blackburn, G. M. (2006). The structure of H5N1 avian influenza neuraminidase suggests new opportunities for drug design. *Nature*, 443(7107), 45-49
- Ryu, Y. B., Kim, J. H., Park, S. J., Chang, J. S., Rho, M. C., Bae, K. H. (2010). Inhibition of neuraminidase activity by polyphenol compounds isolated from the roots of *Glycyrrhiza uralensis*. *Bioorganic & Medicinal Chemistry Letters*, 20(3), 971-974
- Sharma, G., Chowdhury, S., Sinha, S., Majumder, H. K., & Kumar, S. V. (2014). Antileishmanial activity evaluation of bis-lawsone analogs and DNA topoisomerase-I inhibition studies. *Journal of Enzyme Inhibition and Medicinal Chemistry*, 29(2), 185-189
- Singh, S., Jedrzejewski, M. J., Air, G. M., Luo, M., Laver, W. G., & Brouillette, W. J. (1995). Structure-Based Inhibitors of Influenza-Virus Sialidase - a Benzoic-Acid Lead with Novel Interaction. *Journal of Medicinal Chemistry*, 38(17), 3217-3225
- Skehel, J. J., & Wiley, D. C. (2000). Receptor binding and membrane fusion in virus entry: the influenza hemagglutinin. *Annu Rev Biochem*, 69, 531-569. doi: 69/1/531 [pii]

- Stephenson, I., Democratis, J., Lackenby, A., McNally, T., Smith, J., Pareek, M. (2009). Neuraminidase Inhibitor Resistance after Oseltamivir Treatment of Acute Influenza A and B in Children. *Clinical Infectious Diseases*, 48(4), 389-396
- Stoll, V., Stewart, K. D., Maring, C. J., Muchmore, S., Giranda, V., Gu, Y. G. Y. (2003). Influenza neuraminidase inhibitors: Structure-based design of a novel inhibitor series. *Biochemistry*, 42(3), 718-727
- Sugaya, N., Kohno, S., Ishibashi, T., Wajima, T., & Takahashi, T. (2012). Efficacy, Safety, and Pharmacokinetics of Intravenous Peramivir in Children with 2009 Pandemic H1N1 Influenza A Virus Infection. *Antimicrobial Agents and Chemotherapy*, 56(1), 369-377
- Sugaya, N., & Ohashi, Y. (2010). Long-Acting Neuraminidase Inhibitor Laninamivir Octanoate (CS-8958) versus Oseltamivir as Treatment for Children with Influenza Virus Infection. *Antimicrobial Agents and Chemotherapy*, 54(6), 2575-2582
- Tisseh, Z. N., & Bazgir, A. (2009). An efficient, clean synthesis of 3,3'-(arylmethylene)bis(2-hydroxynaphthathene-1,4-dione) derivatives. *Dyes and Pigments*, 83(2), 258-261
- Varghese, J. N., Mckimmbreschkin, J. L., Caldwell, J. B., Kortt, A. A., & Colman, P. M. (1992). The Structure of the Complex between Influenza-Virus Neuraminidase and Sialic-Acid, the Viral Receptor. *Proteins-Structure Function and Genetics*, 14(3), 327-332
- Wang, G. T., Chen, Y. W., Wang, S., Gentles, R., Sowin, T., Kati, W. (2001). Design, synthesis, and structural analysis of influenza neuraminidase inhibitors containing pyrrolidine cores. *Journal of Medicinal Chemistry*, 44(8), 1192-1201
- Wang, G. T., Wang, S., Gentles, R., Sowin, T., Maring, C. J., Kempf, D. J. (2005). Design, synthesis, and structural analysis of inhibitors of influenza neuraminidase containing a 2,3-disubstituted tetrahydrofuran-5-carboxylic acid core. *Bioorganic & Medicinal Chemistry Letters*, 15(1), 125-128
- Yusuf, M., Konc, J., Sy Bing, C., Trykowska Konc, J., Ahmad Khairudin, N. B., Janezic, D. (2013). Structurally conserved binding sites of hemagglutinin as targets for influenza drug and vaccine development. *Journal of Chemical Information and Modeling*, 53(9), 2423-2436. doi: 10.1021/ci400421e
- Yusuf, M., Mohamed, N., Mohamad, S., Janezic, D., Damodaran, K. V., & Wahab, H. A. (2016). H274Y's Effect on Oseltamivir Resistance: What Happens Before the Drug Enters the Binding Site. *Journal of Chemical Information and Modeling*, 56(1), 82-100
- Zhang, L., Cheng, Y. X., Liu, A. L., Wang, H. D., Wang, Y. L., & Du, G. H. (2010). Antioxidant, Anti-Inflammatory and Anti-Influenza Properties of Components from *Chaenomeles speciosa*. *Molecules*, 15(11), 8507-8517

Scheme and Figures



Scheme 1. Synthesis of bis-lawsone analogs with lawsone and different aromatic aldehydes. R=Phenyl represents different aromatic groups from 1-13

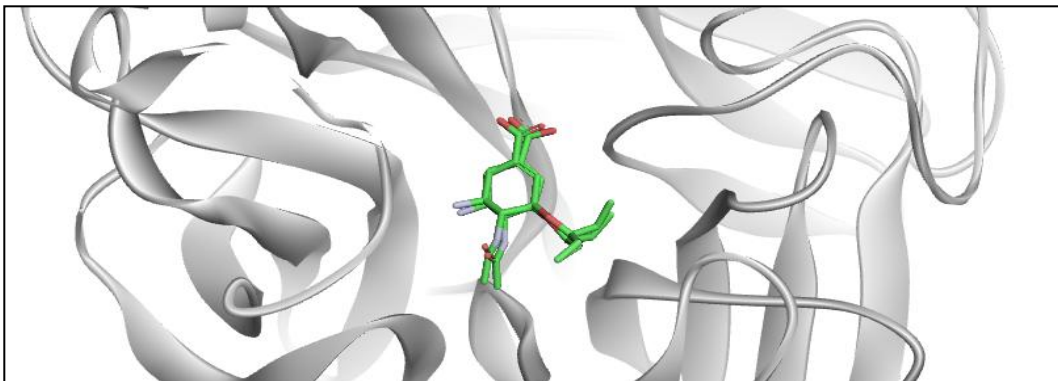


Figure 1. Overlay of the docked ligand with its crystal structure into the active site of the crystal structure of neuraminidase with its co-crystallised ligand in PDB structure(PDB :2HU4) (Russell et al., 2006)

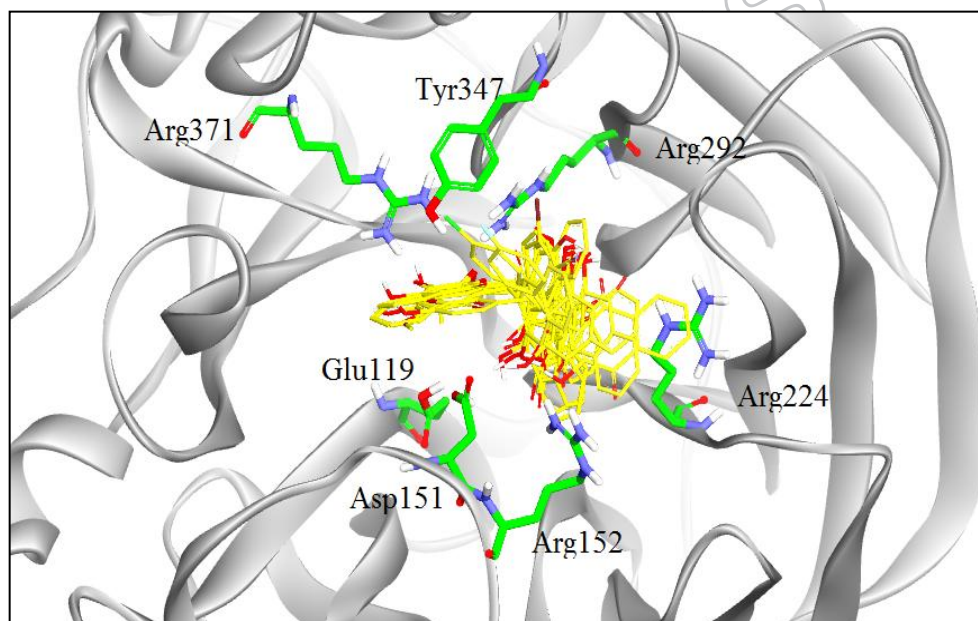
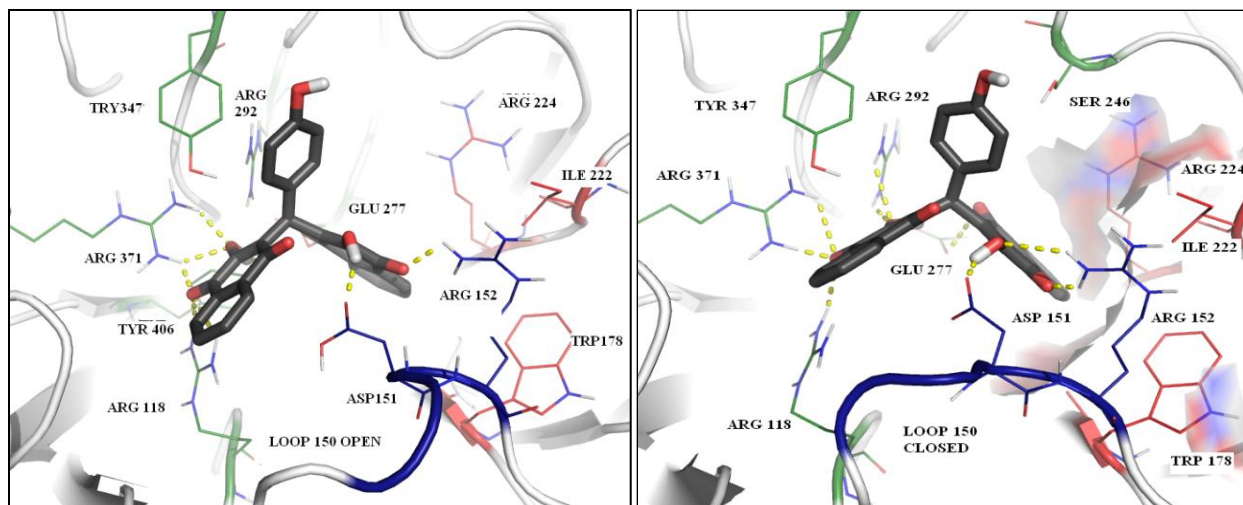


Figure 2. Superimposition of the designed ligands in the binding site of 2HU4



(A)

(B)

Figure 3. Hydrogen bonding of compound-2 (most active compound) with loop 150 open (A) and loop 150 closed (B) (most active compound) with H5N1 neuraminidase. Loop 150 is shown in blue color and hydrogen bonding is in yellow dotted lines. Interaction of amino acid residues with compound 2 with highest score stimulation are shown.

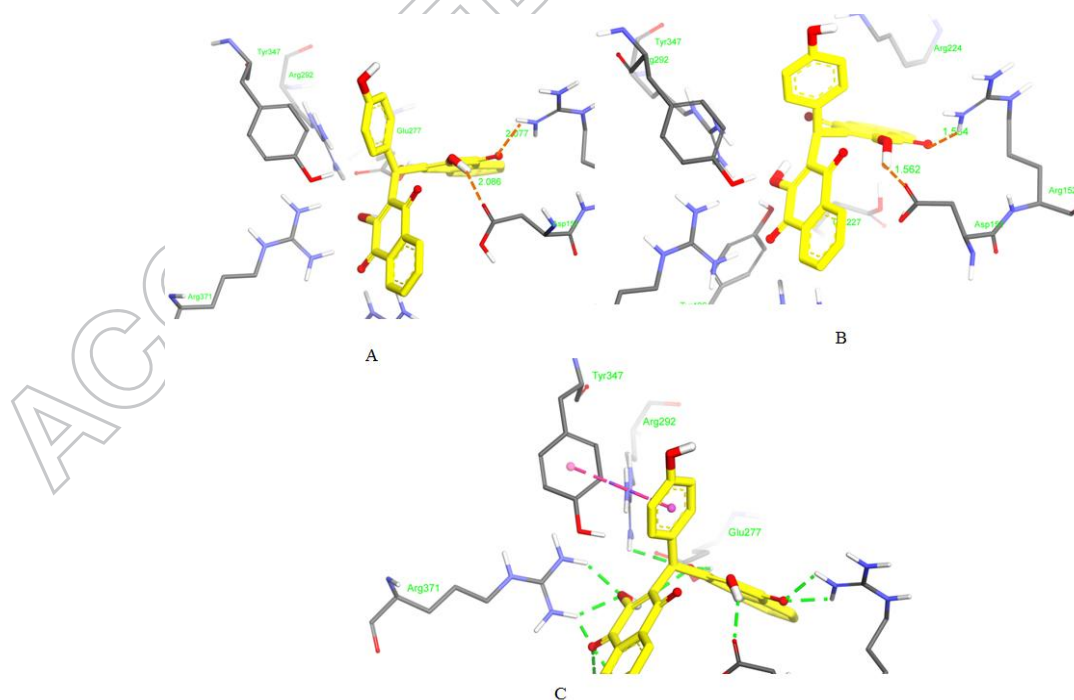


Figure 4. (A) and (B) shows distance of the quinone moiety from Asp 151 and Arg 153. (C) shows the hydrophobic interaction of ligand with Tyr 347

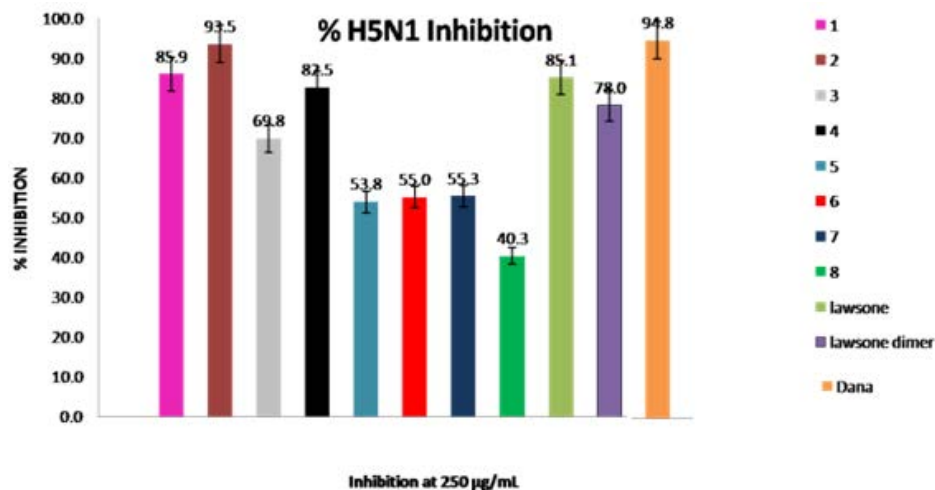


Figure 5. Percentage inhibition of H5N1 NA by the compounds tested. (Inhibition at the highest concentration tested: 250µg/mL)

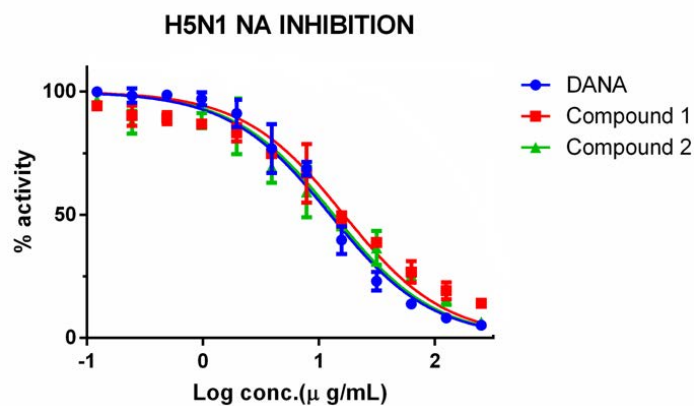
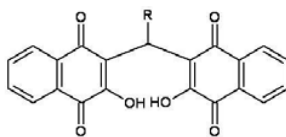


Figure 6. Activity curves for inhibition of compounds 1 and 2 compared to DANA against H5N1 NA. Percentage activity was calculated for compounds 1 and 2 and DANA. Mean activities were measured from three replicate assays for each concentration of compound tested.

Tables

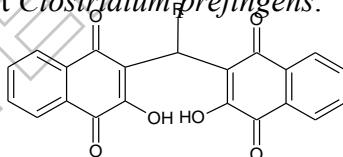
Table 1. The structure of main scaffold with different R groups and the Chemscore of selected ligands.



Compound No.	R=Phenyl	Chemscore ^a
1.	4-OH,3-OCH ₃ -C ₆ H ₃	48.91
2.	4-OH-C ₆ H ₄	50.98
3.	4-OH,3-OC ₂ H ₅ -C ₆ H ₃	46.75
4.	3,4-di-OH-C ₆ H ₃	47.01
5.	3-Br-C ₆ H ₄	46.29
6.	4-CN-C ₆ H ₄	43.80
7.	4-Cl-C ₆ H ₄	40.28
8.	4-F-C ₆ H ₄	38.22

^a Chemscore of all selected ligands in the current study

Table 2. Initial Screening of compounds 1-15 together with lawsone and lawsone dimer at 250 µg/mL against *Clostridium pefingens*.

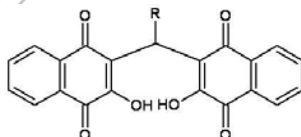


Compound No.	R=Phenyl	% Inhibition
1	4-OH,3-OCH ₃ -C ₆ H ₃	87.8
2	4-OH-C ₆ H ₄	87.0
3	4-OH,3-OC ₂ H ₅ -C ₆ H ₃	89.9
4	3,4-di-OH-C ₆ H ₃	96.6
5	3-Br-C ₆ H ₄	89.9
6	4-CN-C ₆ H ₄	91.2
7	4-Cl-C ₆ H ₄	89.4
8	4-F-C ₆ H ₄	90.0
9	2-Thiophene	81.0

10	3,4,5-tri-methoxy-C ₆ H ₂	78.4
11	4-(N-N-di-methyl amino)-C ₆ H ₄	70.9
12	4-allyloxy-C ₆ H ₄	78.9
13	3,4-di-methoxy-C ₆ H ₃	77.4
14	Lawsone	80.1
15	Lawsone dimmer	85.2
16	DANA	93.0

- Structure of main scaffold where R represents different group
- DANA was used as a standard inhibitor

Table. 3. The structure of main scaffold with different R groups and the corresponding IC₅₀ (μM) values of H5N1 neuraminidase inhibition.



Compound No.	R=Phenyl	IC ₅₀ (μM) ^a
1.	4-OH,3-OCH ₃ -C ₆ H ₃	29 ± 0.9
2.	4-OH-C ₆ H ₄	26.5 ± 0.7
3.	4-OH,3-OC ₂ H ₅ -C ₆ H ₃	252 ± 0.1
4.	3,4-di-OH-C ₆ H ₃	111 ± 0.20
5.	3-Br-C ₆ H ₄	388 ± 0.2
6.	4-CN-C ₆ H ₄	390 ± 2
7.	4-Cl-C ₆ H ₄	425 ± 1
8.	4-F-C ₆ H ₄	N.D
9.	DANA	34.82

^aIC₅₀ ± S.E for each of the compounds tested; DANA was used as standard inhibitor;

Compound 8 (4-F-C₆H₄) not determined (N.D)

ACCEPTED MANUSCRIPT